Supporting Information

Hart et al. 10.1073/pnas.0811457106

SI Text

Generating an Optical Signal; Effect of F175W Mutation on huPrP Folding. The F175W (91–231) huPrP protein expressed at similar levels to wild-type and behaved in the same way during purification in a denaturing 6M GuHCl solution. However, when refolding dialysis was attempted, the protein quickly formed an extensive precipitate. The extent of precipitation was not affected by the method of refolding—an attempt made to refold the protein by rapid dilution into refolding buffer also failed. This inability to fold was also independent of protein length; both the 91–231 and 119–231 constructs failed to fold.

Circular Dichroism. Circular dichroism was measured with a Jasco J-715 spectropolarimeter, using a 1-cm pathlength quartz cuvette. The sample temperature was controlled with a circulating water bath. Far-UV (amide) CD spectra were recorded between 190 nm and 250 nm with 20 μM protein. Near-UV (aromatic) CD spectra were recorded between 250 nm and 310 nm with 70 μM protein. Ten spectra were averaged.

For equilibrium unfolding experiments, 2.5 μM protein was incubated in 20 mM Na_2HPO_4 (pH 8.0) and increasing concentrations of GuHCl. Circular dichroism was recorded at 222 nm.

Fluorescence. Fluorescence was measured by using a 1 × 1-cm pathlength quartz cuvette, and the sample temperature was controlled with a circulating water bath. Fluorescence emission spectra were recorded between 300 and 400 nm with an excitation wavelength of 295 nm, using 2.5 μM protein in 20 mM Na_2HPO_4 (pH 8.0). Ten spectra were averaged.

For equilibrium unfolding, 2.5 μM protein was incubated in 20 mM Na_2HPO_4 (pH 8.0) and increasing concentrations of GuHCl at 21.5 °C. Tryptophan fluorescence emission intensity at 350 nm was measured with an excitation wavelength of 295 nm.

Temperature-Jump. ***Equipment used.*** Folding kinetics were measured by using a Hi-Tech Scientific PTJ-54 temperature jump unit, with a 100-μL quartz sample cell (3-mm pathlength) adapted from a Hi-Tech Scientific SF-51 stopped-flow unit. Kinetic experiments were initiated by a 12-kV electrical discharge across the sample cell. The pretrigger temperature was controlled with a circulating water bath and monitored by a temperature probe adjacent to the sample cell. Samples were directly illuminated with a 75-W mercury-xenon lamp through a 280- to 300-nm bandpass filter. Fluorescence emission was measured via a "highpass" cutoff filter to isolate the optical signal from the sample.

Calibration of system. An *N*-acetyl tryptophanamide (NATA) test solution [50 μM NATA, 200 mM NaCl, 20 mM Na_2HPO_4 (pH 8.0)] was used to measure the response of the instrument to a 12-kV discharge, in terms of size of temperature jump and heating/cooling time. For calibration of jump size, the average fluorescence before and after trigger was measured over 2 ms, with a pretrigger temperature of 15 °C, 20 °C or 25 °C. To measure the time taken for a sample to cool to the initial equilibration temperature after a jump, the fluorescence of the sample was monitored for 15 s, with an initial temperature of 6.6 °C. The effect of GuHCl concentration on the temperature increase was tested by using NATA test solution containing 1, 2, 3, or 4 M GuHCl and a pretrigger temperature of 15 °C. In all cases, 10 kinetic traces were averaged.

Conversion to molar denaturant activity. The equations used to calculate folding parameters from equilibrium unfolding data (described below) assume a linear dependence of the free energy change of protein folding (ΔG) on the concentration of denaturant (1). However, this relationship is known to be nonlinear, particularly at high concentrations of denaturant (2, 3). To allow more accurate extrapolation of data to calculate folding parameters in the absence of denaturant, it is useful to linearize the scale by converting denaturant concentration ([GuHCl]) to molar denaturant activity (D), according to the relationship:

$$D = C_{0.5}[\mathrm{GuHCl}]/(C_{0.5} + [\mathrm{GuHCl}]) \qquad \textbf{[S1]}$$

where $C_{0.5}$ is an empirically derived denaturation constant, which is specific to each denaturant and varies with temperature. For example, for GuHCl at 21.5 °C (the temperature used for kinetics), $C_{0.5}$ = 8.01 (4, 5).

NMR sample preparation and spectroscopy. Expression and purification of ^{15}N-labeled samples of PrP F198W and I184V/F198W constructs for NMR study was carried out as previously described (6). After purification, protein samples were buffer-exchanged into 20 mM sodium acetate-d_3, containing 3 mM sodium azide (pH 5.55) through dialysis, then concentrated in Amicon50 pressure cells to protein concentrations of 0.8–1.2 mM. D_2O (10% vol/vol) was added to the samples to provide the NMR reference signal.

NMR spectra for the assignment of PrP F198W and PrP I184V/F198W were acquired at 303 K on Bruker DRX-500 and DRX-800 spectrometers equipped with 5-mm ^{13}C/^{15}N/^{1}H triple-resonance probes. Two-dimensional sensitivity-enhanced ^{1}H/^{15}N-HSQC (7, 8) spectra were acquired with acquisition times of 163.8 and 87.7 ms in the ^{1}H and ^{15}N dimensions, respectively. Three-dimensional sensitivity-enhanced ^{1}H/^{15}N-TOCSY-HSQC spectra were used to assign side-chain resonances and determine the resonances of the F198W and I184V mutations (8–10). Acquisition times in the 3 dimensions were 102.4 ms (^{1}H directly detected), 16.4 ms (^{15}N), and 14.2 ms (^{1}H indirectly detected). Proton chemical shifts were referenced to 1 mM TSP added to the samples. ^{15}N chemical shifts were calculated relative to TSP, using the gyromagnetic ratios of ^{15}N and ^{1}H (^{15}N/^{1}H = 0.101329118). NMR data were processed and analyzed on Linux workstations using Felix 2004 (Accelrys) software. The modulus of the ^{1}H/^{15}N chemical shift differences (Dmod) was calculated in the following way; Dmod = sqrt((Ddhn)^2 + (Ddn/10)^2), where Ddhn and Ddn are the chemical shift differences in ^{1}H and ^{15}N, respectively.

Amide Exchange-Protection Experiments. Hydrogen–deuterium exchange rates (k_{ex}) were determined by diluting 0.8–1.2 mM ^{15}N-labeled PrP F198W and PrP I184V/F198W samples with an equal volume of 20 mM sodium acetate-d_3, 3 mM sodium azide (pH 5.55) dissolved in 100% D_2O, and acquiring a series of sensitivity-enhanced ^{1}H-^{15}N HSQC spectra (7, 8) at 298 K. The decay curves of the ^{1}H-^{15}N HSQC cross-peaks were fitted to single exponential decays with offset, and protection factors (k_{ex}/k_{int}) for observable amides were determined by using intrinsic exchange rates (k_{int}) (11). Acquisition of the first experiment began ≈3 min after mixing, setting a lower limit on the detection of protection factors of ≈30.

Spin Relaxation Measurements. Spin relaxation measurements (T_1 & T_2) were acquired on ^{15}N-labelled wild type, F198W and I184V/F198W samples as described in ref. 12. Briefly, by using this methodology, heating compensation was improved by the incorporation of a compensation block based on the relaxation

block, followed by a pre-scan ^{1}H saturation sequence and constant length recovery period. Protein concentrations were 0.8–1.2 mM. The T_1 data were obtained using ^{15}N relaxation delays of 40, 80, 140, 240, 370, 570, 730, and 1200 ms. The T_2 data were obtained using ^{15}N relaxation delays of 16, 31, 47, 63, 79, 94, 126, and 240 ms. Spectra were collected with acquisition times of 328 (t2) and 79.2 ms (t1) using 24–64 scans per complex t1 increment.

1. Tanford C (1970) Protein denaturation: Theoretical models for the mechanism of denaturation. *Adv Protein Chem* 24:1–95.
2. Staniforth RA, et al. (1993) The energetics and cooperativity of protein folding: A simple experimental analysis based upon the solvation of internal residues. *Biochemistry* 32:3842–3851.
3. Johnson CM, Fersht AR (1995) Protein stability as a function of denaturant concentration: their thermal stability of barnase in the presence of urea. *Biochemistry* 34:6795–6804.
4. Parker MJ, Spencer J, Clarke A (1995) An integrated kinetic analysis of intermediates and transition states in protein folding reactions. *J Mol Biol* 253:771–786.
5. Parker MJ, et al. (1996) Domain behaviour during the folding of a thermostable phosphoglycerate kinase. *Biochemistry* 35:15740–15752.
6. Hosszu LLP, et al. (2004) The residue 129 polymorphism in human prion protein does not confer susceptibility to CJD by altering the structure or global stability of PrP^{C}. *J Biol Chem* 279:28515–28521.
7. Bodenhausen G, Ruben DJ (1980) Natural abundance N-15 Nmr by enhanced heteronuclear spectroscopy. *Chem Phys Lett* 69:185–189.
8. Schleucher J, et al. (1994) A general enhancement scheme in heteronuclear multidimensional NMR employing pulsed field gradients. *J Biomol NMR* 4:301–306.
9. Palmer AG, et al. (1991) Sensitivity improvement in proton-detected 2-dimensional heteronuclear correlation NMR-spectroscopy. *J Magn Reson* 93:151–170.
10. Kay LE, Keifer P, Saarinen T (1992) Pure absorption gradient enhanced heteronuclear single quantum correlation spectroscopy with improved sensitivity. *J Am Chem Soc* 114:10663–10665.
11. Bai Y, et al. (1993) Primary structure effects on peptide group hydrogen exchange. *Proteins* 17:75–86.
12. Yip GN, Zuiderweg ER (2005) Improvement of duty-cycle heating compensation in NMR spin relaxation experiments. *J Magn Reson* 176:171–178.
13. Zahn R, et al. (2000) NMR solution structure of the human prion protein. *Proc Natl Acad Sci USA* 97:145–150.

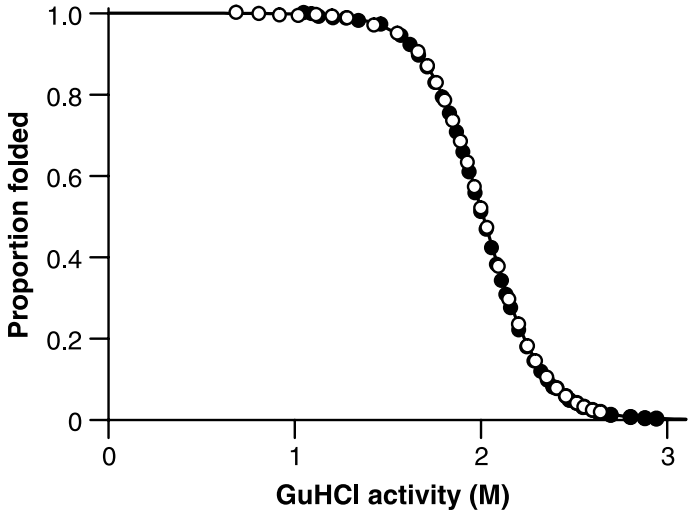

Fig. S1. Equilibrium unfolding of PrP F198W (119–231). GuHCl-induced equilibrium unfolding of human PrP F198W (119–231) was monitored by CD at 222 nm (open circles) or fluorescence at 350 nm (filled circles). Data were obtained at pH 8.0, 21.5 °C, and a protein concentration of 2.5 μM. Data were fitted to a 2-state model of folding (only the fit to CD data are shown, for clarity).

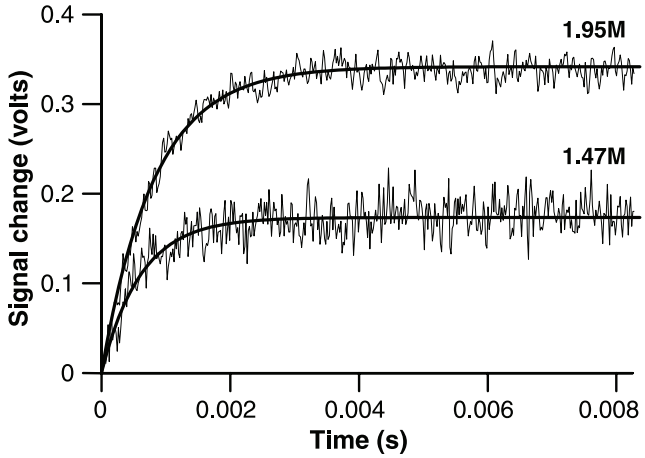

Fig. S2. Relaxation transients of PrP F198W. PrP F198W (119–231) relaxation transients at denaturant activities of 1.47 and 1.95 M. This corresponds to GuHCl concentrations of 1.8 and 2.57 M, respectively. Transients are typically averages of 30 experiments and were recorded with 30 μM PrP, at pH 8.0 and after a 12-kV jump from 15 °C to 21.5 °C. Each data set has been fitted to a single exponential equation.

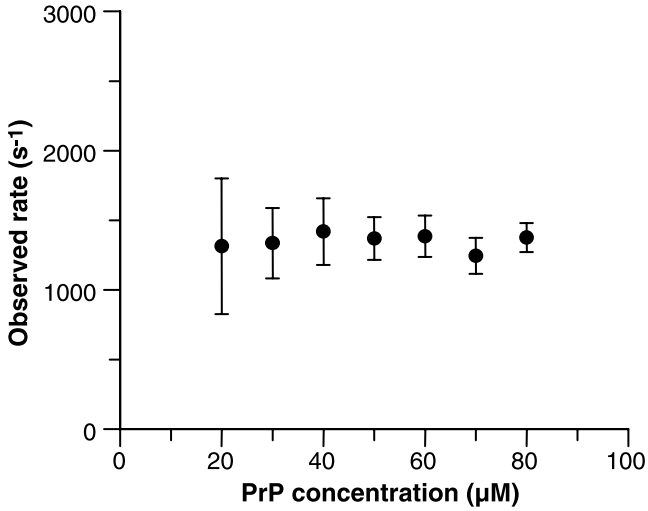

Fig. S3. The effect of protein concentration on I184V observed kinetics. Human PrP F198W/I184V (119–231) kinetics were monitored at 21.5 °C and pH 8 at a GuHCl concentration of 1.65 M (1.37 M GuHCl activity), with a protein concentration from 20 to 80 μM. Relaxation rates shown were calculated from averaged traces by using a single-exponential function.

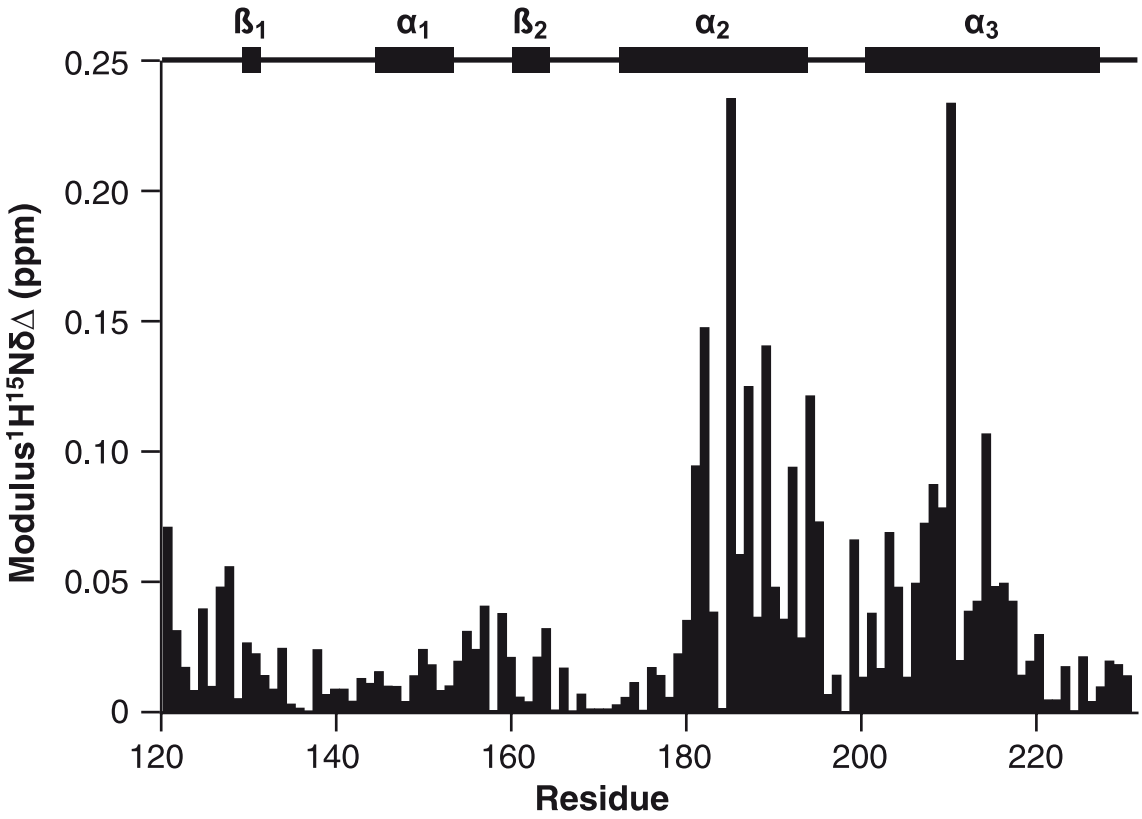

Fig. S4. Perturbation of chemical shifts. $^{1}H/^{15}N$ chemical shift differences between PrP F198W and PrP I184V/F198W at pH 5.5 and 30 °C. A weighted average of both ^{1}H and ^{15}N shift changes are shown, taking into account the difference in the gyromagnetic ratios of ^{1}H and ^{15}N (see *Materials and Methods*). Residues 184 and 198 have been excluded from the figure. Regions of secondary structure in human PrP are denoted at the top of the figure by bars (6, 13).

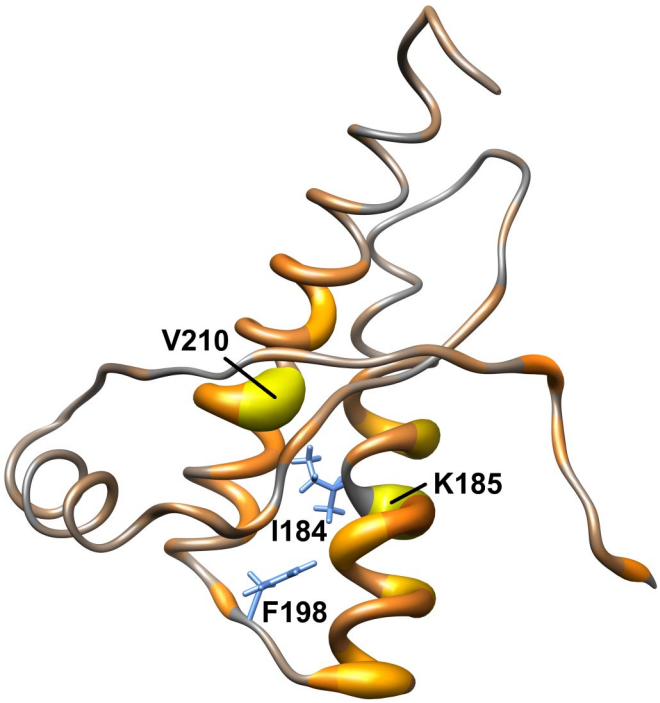

Fig. S5. Location of chemical shift perturbations. Differences in $^{1}H/^{15}N$ chemical shift between PrP F198W and PrP I184V/F198W (see Fig. S4) illustrated on the NMR structure of human PrP^{C} by color (gray → orange → yellow) and width of the backbone structure.

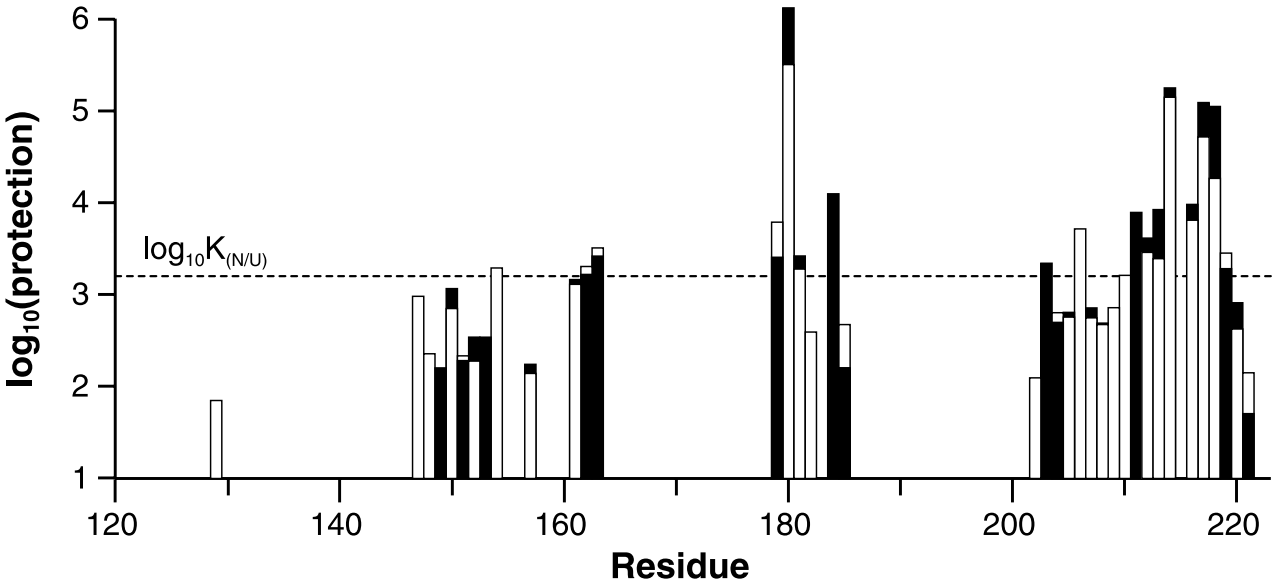

Fig. S6. Hydrogen-exchange protection; effect of the I184V mutation. Amide protection factors (k_{ex}/k_{int}) in PrP F198W (black bars) and PrP I184V/F198W (white bars) for those residues with measurable protection. (Those additional residues that do not appear in both sets of data are due to peak overlap in either set, which precluded measurement of those peaks.) The protection factor corresponding with the equilibrium constant between the native (N) and unfolded (U) states of the protein is plotted as a dashed line ($\log_{10}K_{(N/U)}$). Regions of highest protection surround the disulfide bond that links helices 2 and 3 and that forms a core of residual structure in what is believed to be the unfolded state of the protein.

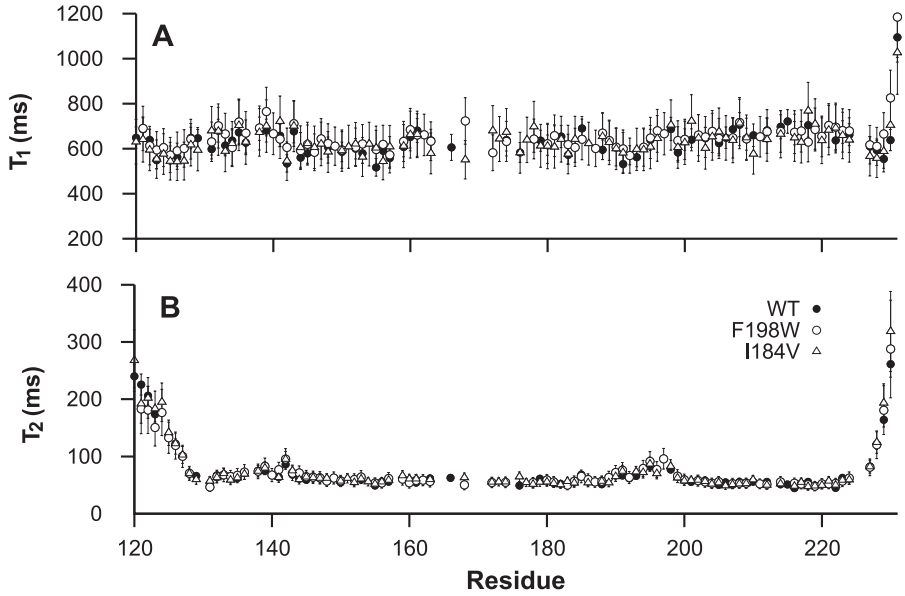

Fig. S7. Dynamics data used to assess the mobility of wild type (filled circles), F198W (open circles), and F198W/I184V (I184V) (open triangles). Longitudinal (T_1) (*A*) and transverse T_2 (*B*) ^{15}N spin relaxation times are shown.

Table S1. Thermodynamic parameters of wild-type and F198W PrP

PrP variant	ΔG, kJ/mol	m, kJ mol^{-1} M^{-1}	Midpoint (molar activity)
Wild-type (91–231) CD	−31.57 ± 0.19	−6.57 ± 0.04	1.96 ± 0.02
F198W (91–231) CD	−30.30 ± 1.23	−6.23 ± 0.25	1.99 ± 0.01
F198W (119–231) CD	−31.43 ± 0.29	−6.27 ± 0.11	2.05 ± 0.03
F198W (119–231) fluorescence	−30.99 ± 0.85	−6.32 ± 0.16	2.00 ± 0.01

Thermodynamic parameters of wild-type human PrP (91–231) and the variants F198W (91–231) and F198W (119–231) at pH 8.0 and 21.5 °C were calculated by using a 2-state model from GuHCl-induced equilibrium unfolding transitions, monitored by either CD at 222 nm or fluorescence at 350 nm, as indicated. The free energy of folding (ΔG) represents the free energy change of folding in the absence of denaturant. The folding midpoint is expressed as molar denaturant activity as described in the text.